An InGaAs P-i-N Photodiode Model: Description and Implementations in the Analysis of the 1.55 μm Lightwave System

M. Cvetković, P. Matavulj, J. Radunović, and A. Marinčić

Abstract— **Using a detailed model of the InGaAs P-i-N photodiode that includes effects caused by the change of bias voltage and effects of the RC parasitic constant, authors describe the implementation of the pulse response of the P-i-N photodiode in the lightwave system model obtaining greater accuracy in comparison to an ideal square-law detector or to the simplified one-pole P-i-N photodiode model. Developed method has been used for the evaluation of the 10 Gb/s 1.55 μm IM/DD (Intensity Modulation/Direct Detection) digital optical system performance with InGaAs P-i-N photodiode as an optical receiver. The authors also propose the correction factor, the photodiode bandwidth penalty, in the total optical system penalty that describes the influence of the P-i-N photodiode properties on the optical system performance.**

Keywords— **Lightwave system, linear response, optical communication, P-i-N photodiode, system penalty.**

I. Introduction

ON E of the key issues in the research and analysis of the high bit rate optical communication systems are the behaviour and performance of the optical photodiodes. Among various types of photodiodes, P-i-N photodiodes represent the common devices that are used in the nowadays lightwave systems due to their high reliability, low cost and relatively simple process of fabrication.

The optical photodiodes are often considered in the analysis of the lightwave systems as a devices with approximated characteristics, i.e. with infinite bandwidth or with simplified transfer function, even in detailed analysis of the complete lightwave systems [1]-[3]. However, their specific properties such as the nonlinearity or finite bandwidth require thorough analysis.

Various papers in the recent past deal with the specific properties of the P-i-N photodiodes [4]-[12]. Most of the P-i-N photodiode mathematical models are based on the standard continuity equations for the carriers in the active volume. Starting from these equations, there are two basic approaches in the characterization of the P-i-N photodiode output response. The first approach is based on the derivation of the photodiode output response as a function of the photodiode input signal. The output response can by obtained analytically (e.g. see Sabela et al. [7]) or numerically (e.g. see Williams et al. [10]) depending on the level of model complexity and usage of various mathematical methods. Although these approaches can be useful for the implementations in the modeling of the P-i-N photodiode as a part of the optical communication system, its derivation may require the negligence of the various photodiode characteristics. The second approach is based on the derivation of the P-i-N photodiode pulse response that can give valuable informations about photodiode characteristics. Using this technique, it was possible to study nonlinear behaviour of the P-i-N photodiode caused by the space charge effects due to photogenerated carriers [5], or caused by the change of bias voltage [11], or to analyze the P-i-N photodiodes based on the two-valley semiconductor [9], [12].

Although the P-i-N photodiode in general has the nonlinear pulse response, it can be numerically shown that its pulse response can be treated as linear for the low level of incident light energy without loosing the impact of the relevant photodiode effects. This enables the implementation of the P-i-N photodiode pulse response in the development of the mathematical model for the optical communication systems, where the output signal from the optical fiber and input signal for the electrical filter/amplifier at the receiver side represent photodiode input and output signal, respectively.

To illustrate the described approach, we have implemented the P-i-N photodiode model derived in [11] in the model of the 1.55 μm IM/DD (Intensity Modulation/Direct Detection) optical communication systems due to their spreadness and relatively simple structure. We consider InGaAs P-i-N photodiode including the properties such as RC parasitic constant and effects caused by the change of bias voltage. Although this model does not take into account the other P-i-N photodiode properties such as the change of the electric field caused by space charge of photogenerated carriers and nonstationary effect caused by electron intervalley transfer [12], the model is able to explain the dynamics of the photodiode as the part of a ligtwave system.

Paper is organized as follows. Developed model described in section II includes all the relevant components of the typical IM/DD digital optical communication system. The results from the computer simulation of the lightwave system with special emphasis on the InGaAs P-i-N photodiode performance are presented in section III, while the summary and conclusion are given in section IV.

M. Cvetković is with the Faculty of Technology and Metallurgy, University of Belgrade, P.O.Box 35-03, Karnedžijeva 4, 11120 Belgrade, Yugoslavia

P. Matavulj, J. Radunović and A. Marinčić are with the Faculty of Electrical Engineering, University of Belgrade, P.O.Box 35-53, Bulevar revolucije 73, 11120 Belgrade, Yugoslavia, E-mail: p.matavulj@ieee.org

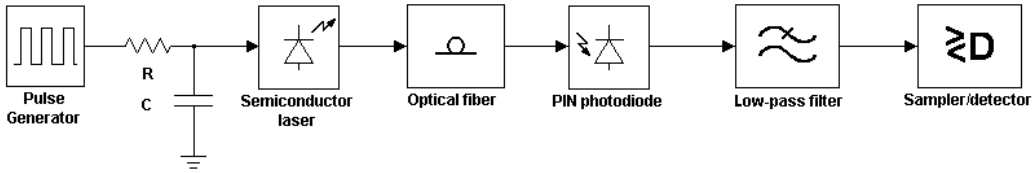

Fig. 1. Schematic representation of the analyzed lightwave system.

II. Description of the model

In our analysis we consider 1.55 μm IM/DD lightwave system that consists of a transmitter, optical fiber and receiver. The lightwave system is schematically depicted in Figure 1. Single-mode semiconductor laser diode is considered as an optical transmitter. The signal is then propagated through the single-mode optical fiber. Optical receiver consists of the P-i-N photodiode and the electric filter placed before sampling/detector unit. We assume that the optical amplifier/filter unit that may precede the P-i-N photodiode has unlimited bandwidth and constant amplification, and therefore, we do not include it in the model. We also omit the coupling loss of the laser diode and optical fiber, as well as the coupling loss of the optical fiber and P-i-N photodiode.

While the laser diode is modeled with standard rate-equations, single-mode optical fiber, P-i-N photodiode and electrical filter are modeled with appropriate pulse responses of these devices. The output signal from each of these devices is obtained by calculating the convolution of the input device signal and the appropriate device pulse response. This approach assumes that optical fiber, P-i-N photodiode and electrical filter can be considered as a linear devices. Comparing to the Fourier transform implementation (e.g. the calculation of the optical fiber output response in [14]), the calculation in the time domain does not require the complete knowledge of the input signal, which makes this approach useful for the behaviour study or circuit modeling of the lightwave systems [16], [17].

A. Transmitter

The laser diode is modeled using the spatially averaged rate equations that can be found in a similar form elsewhere in the literature [1], [2], [16]:

$$\frac{dn}{dt} = \frac{I_b(t)}{Ve} - v_g \frac{G_n(n-n_0)}{1+\varepsilon s} - R(n) \tag{1}$$

$$\frac{ds}{dt} = \Gamma v_g \frac{G_n(n-n_0)}{1+\varepsilon s} - \frac{s}{\tau_{ph}} + \frac{R_{sp}}{V} \tag{2}$$

$$\frac{d\Phi}{dt} = \frac{\alpha_L}{2}\left[\Gamma v_g G_n(n-n_0) - \frac{1}{\tau_{ph}}\right] \tag{3}$$

where n and s are the average density of carriers and photons, respectively, in the laser diode active zone, $\Phi(t)$ is the phase of the electric field, $I_b(t)$ is the laser diode bias current, $R(n)$ is the spontaneous recombination rate of the carriers, while e is electron charge. Other laser diode parameters are described in table I. It should be noted that the equation (3) is given in form like in [2]. We assume that the spontaneous recombination rate is in the standard polynomial form

$$R(n) = A_r n + B_r n^2 + C_r n^3 \tag{4}$$

where the coefficients are defined in table I.

The laser diode parasitics are modeled as a series resistance and parallel capacitance similarly to [1]:

$$\frac{dI_b}{dt} = \frac{I_d - I_b}{\tau_L} \tag{5}$$

where $I_d(t)$ is the laser diode driver current and τ_L is the laser diode parasitics circuit time constant. The output power per one facet $P(t)$ of the laser diode is given by

$$P(t) = \frac{\eta h \nu V s}{2\Gamma\tau_{ph}} \tag{6}$$

where ν is the optical frequency, η is differential quantum efficiency and h is the Planck constant.

B. Optical fiber

We assume that the laser diode output signal is ideally coupled with optical fiber. Envelope of the input electrical field of the signal injected into the optical fiber is of the form

$$E_{in}(t) = \sqrt{P(t)} e^{j\Phi(t)}. \tag{7}$$

If we omit the Kerr effect during the propagation of the signal in the fiber, i.e. if we assume that the input optical power into the fiber is less then 10 mW (e.g. see [13]), the pulse response of the 1.55 μm single-mode optical fiber is given by [2]

$$h_f(t) = \sqrt{\frac{c}{2\lambda^2 DL}}(1-j) e^{-j\frac{\pi c t^2}{\lambda^2 DL}} \tag{8}$$

where c is the light velocity in vacuum, D is the fiber dispersion, L is the fiber length and λ is the optical wavelength.

The output optical power from the fiber is given by [15]

$$P_f(t) = A_f |E_{in}(t) * h_f(t)|^2 \tag{9}$$

where A_f is the fiber attenuation, while operation $*$ denotes convolution.

C. Receiver

The electric circuit of the photodiode used for detection is shown in Figure 2. The detected signal is $U_R(t)$, and $U(t)$ is the voltage of the reverse biased P-i-N photodiode, $I(t)$ is its photocurrent and R the load resistance, while V_{cc} is the bias voltage.

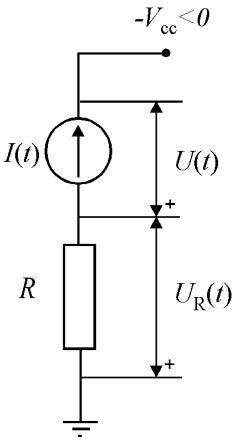

Fig. 2. Electric circuitry of P-i-N photodiode.

In the equivalent circuit of the photodiode the resistance of the diode contacts and parasitic capacitance of the external circuitry are omitted, while the P-i-N photodiode capacitance is taken into account via the displacement current. During the detection of the incident radiation, the photodiode generates photocurrent which causes a voltage drop on the load resistance, and thus changes the photodiode voltage:

$$U(t) = V_{cc} - U_R(t) = V_{cc} - RI(t). \tag{10}$$

This causes a perturbation of the electric field controlling the carriers transport, inducing in turn photocurrent to change and nonlinearity effects to appear.

In our analysis we consider an InGaAs P-i-N photodiode. The effects of the space charge due to photogenerated carriers are omitted. In such case the electric field perturbation in the depletion region is caused only by the change of bias voltage. We assume the semiconductor doping level in the i-region to be low, so that the electric field in this region is homogeneous. We also assume that the length of the i-region is much larger than that of p- and n-regions, therefore the photon absorption in the latter two regions, and hence the diffusion currents, may be neglected. Finally, the reverse bias voltages are assumed not to be very high, and we can assume that mobility of the holes and electrons μ_p and μ_n, respectively, are constant. We also omit recombination and thermal generation in the appropriate continuity equations for electrons and holes.

We assume that the pulse response of the P-i-N photodiode is induced by the power of the incident radiation $P_f(t)$ given by

$$P_f(t) = W\delta(t) \tag{11}$$

where W is the energy of the incident radiation. Since the pulse response of the P-i-N photodiode and its nonlinearity are dependent on W, we consider the P-i-N photodiode pulse response h_{ph} as the function of two variables: time t and energy of the incident radiation W.

Under all these assumptions and after transforming and solving the set of basic P-i-N photodiode equations, the pulse response of the P-i-N photodiode $h_{ph}(t, W)$ for $t \geq 0^+$ is given by [11]:

$$h_{ph}(t, W) = V_{cc} - V_D - V(t, W) \tag{12}$$

where V_D is the punch-through voltage, and $V(t, W)$ is given in the implicit form as

$$-t = Y \ln \left| \frac{V(t,W) - \frac{Z}{X}}{V(0^+,W) - \frac{Z}{X}} \right| - X \ln \left| \frac{V(t,W)}{V(0+,W)} \right| + Z \left(\frac{1}{V(t,W)} - \frac{1}{V(0^+,W)} \right), \; 0^+ \leq t \leq t_{cn} \tag{13}$$

$$-(t - t_{cn}) = Y_1 \ln \left| \frac{V(t,W) - \frac{Q}{X_1}}{V(t_{cn},W) - \frac{Q}{X_1}} \right| - X_1 \ln \left| \frac{V(t,W)}{V(t_{cn},W)} \right| + Q \left(\frac{1}{V(t,W)} - \frac{1}{V(t_{cn},W)} \right), \quad t_{cn} \leq t \leq t_{cp} \tag{14}$$

$$V(t,W) = (V_{cc} - V_D) + [V(t_{cp},W) - (V_{cc} - V_D)] e^{\frac{-t - t_{cp}}{\tau}}, \quad t_{cp} \leq t < +\infty. \tag{15}$$

Symbols τ, Z, Q, X, X_1, Y, and Y_1 from (13)-(15) are given by

$$\tau = \frac{R\varepsilon S}{d}, \; Z = \frac{a_1^2 + a_2^2}{\alpha a_1 a_2 (a_1 - a_2)}, Q = \frac{1}{\alpha a_2},$$

$$X = \frac{C}{V_{cc} - V_D} Z, \; X_1 = \frac{C_1}{V_{cc} - V_D} Q, \; Y = \frac{\tau}{C} + X,$$

$$Y_1 = \frac{\tau}{C_1} + X_1$$

respectively. In above definitions, ε, S, d and α are explained in table I, while a_1, a_2, C and C_1 are given by

$$a_1 = \frac{\mu_n}{d}, \; a_2 = \frac{\mu_p}{d}, \; C = 1 + Aa_1 - Aa_2 e^{-\alpha d},$$

$$C_1 = 1 - Aa_2 e^{-\alpha d}$$

respectively, and

$$A = \frac{Re\lambda W}{hcd}$$

Time boundaries t_{cn} and t_{cp} from (13)-(15) denote the time in which all electrons leave the depletion region and the

time in which all holes leave depletion region, respectively. The values of t_{cn} and t_{cp} are defined by the relations

$$\int_0^{t_{cn}} V(t,W)\,dt = \frac{d}{a_1},\ \int_{t_{cn}}^{t_{cp}} V(t,W)\,dt = d\frac{a_1-a_2}{a_1a_2}. \quad (16)$$

Finally, the boundary voltage $V(0^+,W)$ is defined by

$$V(0^+,W) = \frac{V_{cc}-V_D}{1+A(a_1+a_2)(1-e^{-\alpha d})} \quad (17)$$

while $V(t_{cn},W)$ and $V(t_{cp},W)$ are defined by equations (13) and (14), respectively.

The set of equations (12)-(17) implicitly defines the P-i-N photodiode pulse response $h_{ph}(t,W)$ that can be calculated numerically. It has been shown in [11] that the P-i-N photodiode is a nonlinear device for high values of incident optical energy W. However, if the level of the incident optical energy is small, the P-i-N photodiode can be considered as a linear device. This assumption enables the implementation of the convolution for the calculation of the time domain response. Since the photodiode pulse response cannot be expressed analytically, it is convenient to calculate the convolution integral numerically at equidistant points. Hence, the output signal from the P-i-N photodiode (load voltage) $U_R(kT_s)$ is given by

$$U_R(kT_s) = \sum_{i=0}^{+\infty} \frac{P_f(iT_s)}{W_s} h_{ph}((k-i)T_s, W_s)T_s, k \geq 0 \quad (18)$$

where T_s is the sampling rate and W_s is the nominal energy of the incident radiation. The introduction of W_s is possible since the P-i-N photodiode may be considered as a linear device. In equation (18), we assume that $P_f(t) = 0$ and $h_{ph}(t,W_s) = 0$ for $t < 0$.

After photodetection, the photodiode output signal has to be filtered before the regeneration of the digital signal is committed by sampler/detector unit. The output electrical signal $U_b(t)$ from the filter is given by

$$U_b(t) = U_R(t) * h_b(t) \quad (19)$$

where $h_b(t)$ is the filter pulse response.

The set of equations (1)-(19) fully defines the propagation of the signal through IM/DD lightwave system and represents the basis for the computer simulation of this type of optical communication systems.

III. Results and discussion

Typical pulse responses $h_{ph}(t,W)$ of the P-i-N photodiode for the different values of energy of the incident radiation W are shown in Figure 3. The parameters for the InGaAs P-i-N photodiode, are taken from [10] and shown in Table I, as well as the parameters for other optical components, while the thickness of the i-region is held constant at $d = 3\mu$m. The similar set of parameters has been used in [21] where we presented the modeling of the basic optical system properties.

One can notice that load voltage remains almost unchanged until all the electrons leave the depletion region (for $W = 100$ fJ at $t = t_{cn} \approx 5$ ps). After that, the holes become the dominant component in the current which significantly decreases the load voltage. When all the holes leave the depletion region (for $W = 100$ fJ at $t = t_{cn} \approx 75$ ps), the displacement current becomes the dominant component in current and the load voltage drops exponentially.

TABLE I
Parameters used in computer simulation.

Laser Diode Parameters [13]	**Symbol**	**Value**
Active zone volume	V	$1.53 \cdot 10^{-17}\,\mathrm{m}^3$
Confinement factor	Γ	0.06
Linewidth enhancement factor	α_L	3
Photon lifetime	τ_{ph}	1.9 ps
Nonradiative recombination	A_r	$10^8\ \frac{1}{\mathrm{s}}$
Radiative recombination	B_r	$1.5 \cdot 10^{-16}\ \frac{\mathrm{m}^3}{\mathrm{s}}$
Auger recombination	C_r	$4.5 \cdot 10^{-41}\ \frac{\mathrm{m}^6}{\mathrm{s}}$
Transparent carrier density	n_0	$1.307 \cdot 10^{24}\ \frac{1}{\mathrm{m}^3}$
Spontaneous emission rate	R_{sp}	$10^{12}\ \frac{1}{\mathrm{s}}$
Group velocity	v_g	$8.33 \cdot 10^7\ \frac{\mathrm{m}}{\mathrm{s}}$
Differential gain	G_n	$6.5 \cdot 10^{-20}\ \mathrm{m}^2$
Nonlinear gain coefficient	ε	$4 \cdot 10^{-23}\ \frac{1}{\mathrm{m}^3}$
Differential quantum efficiency	η	0.2
Laser diode parasitic time constant	τ_L	15 ps
Fiber Parameters[13]	**Symbol**	**Value**
Fiber attenuation	A_f	$0.22\ \frac{\mathrm{db}}{\mathrm{km}}$
Fiber dispersion	D	$16\ \frac{\mathrm{ps}}{\mathrm{nm \cdot km}}$
Photodiode parameters [10]	**Symbol**	**Value**
Absorption coefficient	α	$1.15 \cdot 10^3\ \mathrm{cm}^{-1}$
P-i-N active area	S	$700\ \mu\mathrm{m}^2$
Width of the i-region	d	2.5-6 μm
Mobility of electrons	μ_n	$0.8\ \frac{\mathrm{m}^2}{\mathrm{Vs}}$
Mobility of holes	μ_p	$0.03\ \frac{\mathrm{m}^2}{\mathrm{Vs}}$
Load resistance	R	30 Ω
Punch-through voltage	V_D	0.6 V
Bias voltage	V_{cc}	5 V
Relative dielectric permitivity	ε_r	13.67

It is of special interest to determine the conditions when the photodiode pulse response $h_{ph}(t)$ can be considered as a linear. Numerical analysis has shown that the characteristic values t_{cn} and t_{cp} remains practically constant for $W < 10$ fJ, while the increase of W causes the rise in t_{cn} and t_{cp}. Hence, the linearity can be expected only when the energy of incident radiation is $W < 10$ fJ. Figure 4 approves the latter conclusion. Relative change of t_{cn} and t_{cp} becomes significantly high for $W > 10$ fJ. However, the decrease of the i-region width d also causes the rise of t_{cn} and t_{cp} and yields the nonlinear behaviour of the photodiode. Physically, this can be explained with a fact that the model does not take into account the saturation of the electron velocity v_n and holes velocity v_p. For the given set of photodiode parameters, the nonlinearity occurs for the i-region width smaller than 2.5 μm. This represents the other constraint for the implementation of the photodiode pulse response.

The latter analysis enables us to consider the implementation of the described P-i-N photodiode model as the part in the full model of the lightwave system. To investigate this option, we modify the model [16] for the 10Gb/s IM/DD lightwave system (pulsewidth T=100 ps) that is de-

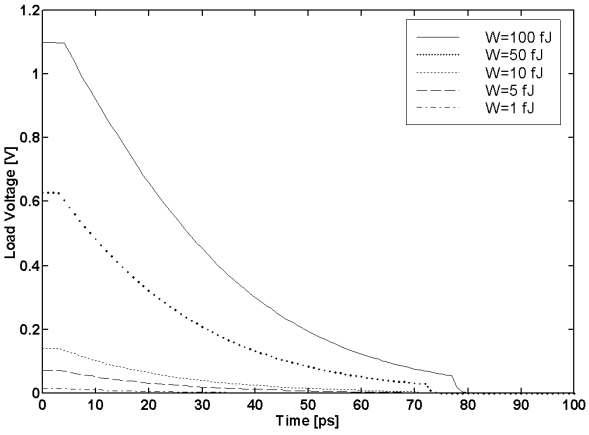

Fig. 3. Pulse response of the InGaAs P-i-N photodiode for different values of W. The thickness of the i-region is $d = 3\mu m$.

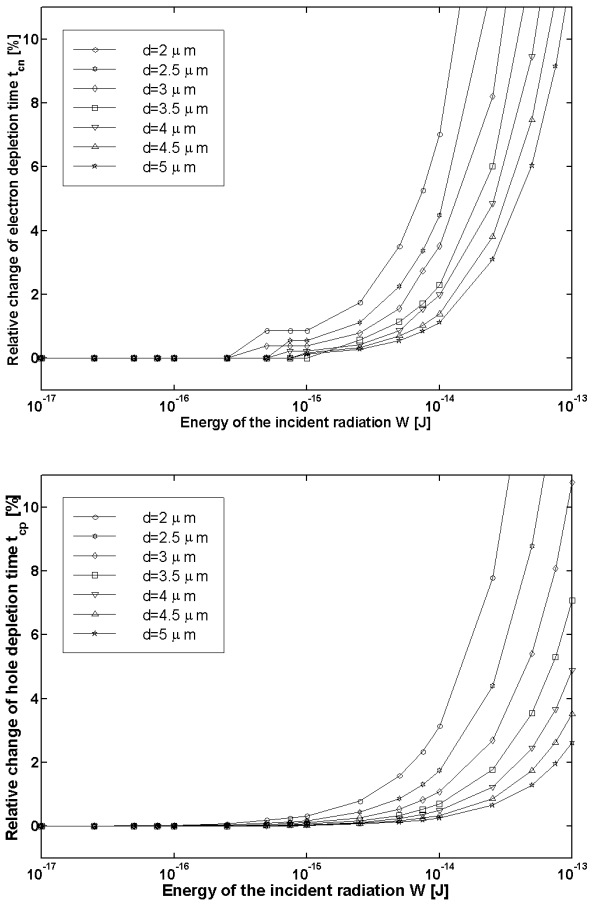

Fig. 4. Relative change of the electron depletion time t_{cn} and hole depletion time t_{cp} versus energy of the incident radiation W.

scribed in [13] by introducing the P-i-N photodiode at the receiver side instead of an ideal square-law detector. Under these assumptions, the IM/DD system has the structure like in Figure 1. The laser diode and the optical fiber parameters used in simulation are taken from [13] and shown in Table I.

The input signal into the lightwave system is considered to be a NRZ (Not-Return-to-Zero) 10 Gb/s digital signal generated as a $2^8 - 1$ pseudorandom bit sequence. The laser diode behaviour is described with the equations (1)-(3). Similarly to [16], we take into account the bit shape in the input signal and the laser diode parasitics.

The electric field of the output optical signal from the laser diode is then coupled with the optical fiber. Since the pulse response of the fiber is not a finite function in a numerical calculation, the usage of the window function is essential for the correct calculation of the output optical signal of the fiber given by (9). We have used the Hamming-like window function described in [17] to truncate the fiber pulse response. Accuracy of the approximation depends also on the sampling rate T_s and the number of samples n_f taken from the fiber pulse response. Discussion concerning the determination of the optimal values of n_f and T_s can be found elsewhere [16], [17], [20]. In our analysis, the fiber pulse response is approximated with $n_f = 1000$ samples taken with the sampling rate $T_s = 1$ ps, which should provide satisfying accuracy of the calculation and be in agreement with the analysis from the literature.

The output signal from the optical fiber is convoluted with the P-i-N photodiode pulse response $h_{ph}(t)$. Photodiode pulse response $h_{ph}(t, W_s)$ is calculated at $n_{ph} = 250$ sampling points with the sampling rate $T_s = 1$ ps (sampling rate for the pulse responses of the optical fiber and photodiode must be the same) and nominal energy of incident radiation $W_s = 1$ fJ. These values of parameters are justified if the condition $n_{ph}T_s > 1.1t_{cp}$ is fulfilled, since $h_{ph}(t, W_s) \approx 0$ for $t \geq 1.1t_{cp}$. This condition is fully satisfied for the parameters from Table 1. Although the pulse response $h_{ph}(t)$ can be truncated and smoothed using the various window function, we assume that simple square window function is used (i.e. no special window function is used to correct the approximated pulse response). This is justified with the fact that almost whole pulse response $h_{ph}(t, W_s)$ is bounded with $0 < t \leq 1.1t_{cp}$.

Load voltage obtained from the P-i-N photodiode is then filtered using the 2nd order Butterworth filter which cut-off frequency is set to $f_B = 0.65/T = 6.5$ GHz.

Figure 5 shows various dynamic properties of the described optical system. Driver current amplitude is 20 mA while driver bias current is 50 mA (equivalent to extinction ratio 2.75:1). Rise and fall times of the driver pulses are 50 ps, while the laser diode parasitics time constant is $\tau_L = 15$ ps to match the conditions described in [16]. The input electrical signal (Fig. 5a) induces the laser diode chirp (Fig. 5b) and laser diode output optical power $P(t)$ (Fig. 5c). Laser diode chirp and output power define the input signal for optical fiber. Due to laser chirp and fiber dispersion, the propagating signal through the optical fiber starts to deform. Typical output optical power from 50 km long fiber is shown in Fig 5e. It should be noted that Fig. 5a-5c and 5e are very similar to plots from Fig. 1 in [16]. When the InGaAs P-i-N photodiode is placed at the end of laser diode with no fiber between them (Fig. 5d) and

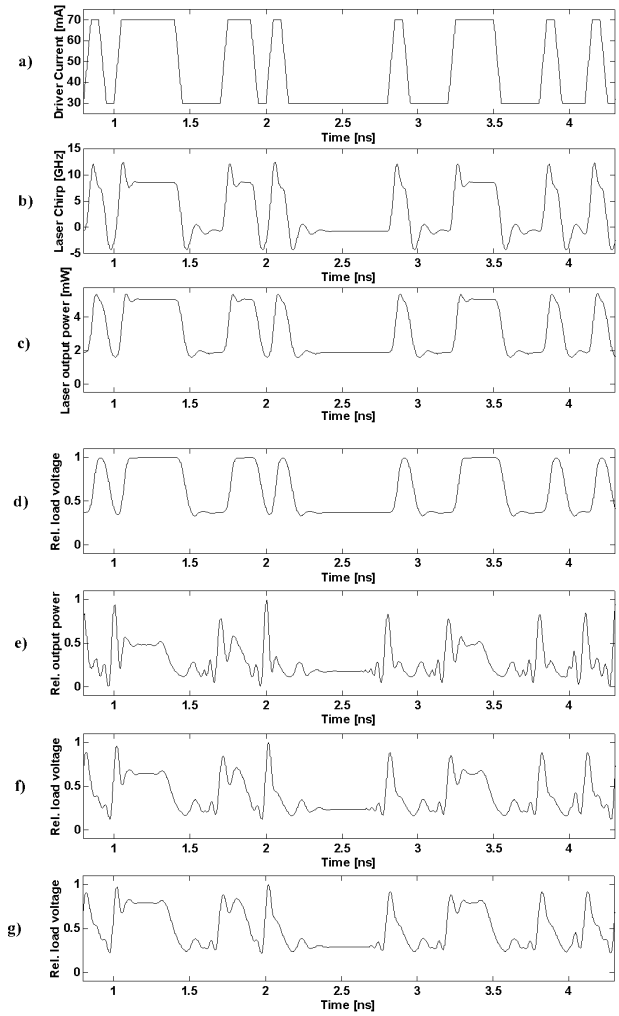

Fig. 5. Various dynamical properties of the lightwave system: laser diode driver current (a), laser diode chirp (b), laser diode output optical power (c), normalized load voltage of the pin photodiode with $d = 3\mu$m and no fiber in place (d), output optical power from the 50km long fiber (e), normalized load voltage of the pin photodiode with $d = 3\mu$m and 50km long fiber in place (f), normalized load voltage of the pin photodiode with $d = 5\mu$m and 50km long fiber in place (g).

at the end of 50km long fiber (Fig. 5f), the shape of the propagating signal is changing due to limited bandwidth of the P-i-N photodiode. When the width of P-i-N photodiode i-region is $d = 3\mu$m (Fig 5d and 5f) the detected differences from Fig. 5c and 5e are minor due to high bandwidth of the P-i-N photodiode. Increasement of d leads to the stronger filtering of the signal like for $d = 5\mu$m and further flattening of the signal "peaks" (Fig. 5g).

The effect of the P-i-N photodiode filtering can be seen even more clearly on the Figure 6 where the eye-diagrams of the output signal from the electric filter are shown for ideal square-law photodiode, P-i-N photodiode with $d = 3\mu$m and P-i-N photodiode with $d = 5\mu$m. Increasement of d leads to the smaller overshoot and stronger filtering in addition to the electric filtering.

Although the Figure 5 depicts the physical relations between the dynamic properties, it does not provide the information about the success of signal transmission and the characterization of its performance. There are two basic approaches in the characterization of transmission. The first is based on the calculation of BER (Bit Error Rate) using the theory of statistical random process [2]. The second approach is based on the measuring of the eye-diagram opening and calculating of the dispersion power penalty given by [18], [19]

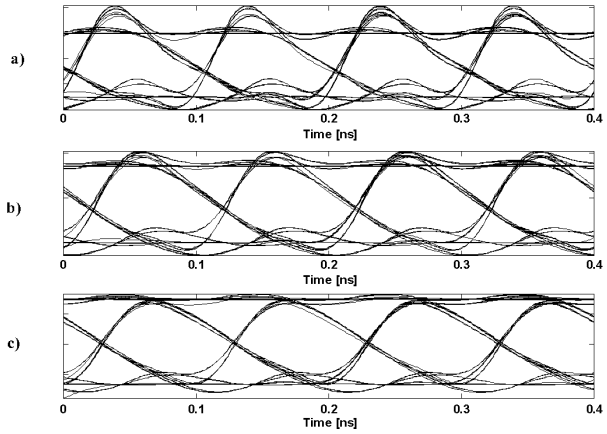

Fig. 6. Eye-diagrams of the output signal from the electric filter with ideal square-law detector (a), P-i-N photodiode with $d = 3\mu$m (b) and P-i-N photodiode with $d = 5\mu$m (c). Length of the optical fiber is 50 km.

$$P_D(L) = 10 \log \frac{y(L)}{y(0)} \tag{20}$$

where $y(L)$ is the eye opening of the optical system with fiber length L assuming that the fiber attenuation $A_f = 0$, while $y(0)$ is the eye opening of the optical system with no fiber in place (i.e. fiber length zero).

Apa rt from the dispersion penalty, the other important penalty component is extinction ratio penalty caused by the existence of non-zero optical power level from the laser diode, and given by

$$P_E = 10 \log \left(\frac{r_{ext} + 1}{r_{ext} - 1} \right) \tag{21}$$

where $r_{ext} = P_1/P_0$ is the extinction ratio defined by the ratio between optical power level of the logical "1" and optical power level of the logical "0" of the laser diode output signal.

System power penalty $P_S(L)$ is usually defined as the sum of the dispersion penalty and extinction ratio penalty i.e. $P_S(L) = P_D(L) + P_E$. System power penalty versus length of the optical fiber is shown in Figure 7 for different values of P-i-N photodiode i-region width d. The interaction of laser diode chirp and fiber dispersion causes the local maximum for fiber length of around 15-20km (near distance) and local minimum for fiber length of around 50-60km (middle distances) due to self-steepening effect

caused by the interaction between adiabatic laser diode chirp and dispersion [1].

When the photodiode is not considered as an ideal square-law detector, the increase of P-i-N photodiode i-region d yields the further decrease in power penalty at middle distances due to stronger filtering. Further increase of d causes negative dispersion penalty when the bandwidth of the P-i-N photodiode becomes lower than the system bit-rate, which is in accordance to [1]. Although one may deduce that the further increase in i-region width d leads to low penalty signal propagation, it should be noted that it yields lower photodiode bandwidth and the degradation of the high bit-rate digital signals.

Since the properties of the P-i-N photodiode (in particular, the photodiode bandwidth) may cause negative dispersion penalty, there is a need for the calculation of their influence and the appropriate power penalty. To correct the expression for the system power penalty we introduce the photodiode bandwidth penalty. This penalty accounts the fact that when the bit-rate of the input digital signal is high, the photodiode will not be able to fully reproduce the output signal due to its limited bandwidth. Assuming that the input signal of the P-i-N photodiode is digital bit sequence of the form "10101010..." with ideally square shaped bits and that the bit rate is B, the photodiode bandwidth penalty is given by

$$P_P = 10 \log \frac{y_P(B)}{y_{Pmax}} \tag{22}$$

where $y_P(B)$ is the eye opening of the P-i-N photodiode with input signal bit rate B and y_{Pmax} is the maximum eye-opening of the P-i-N photodiode (when B is much lower than the P-i-N photodiode bandwidth and the output values of "1"'s an "0"'s reach their stationery values).

Combined dispersion and photodiode bandwidth penalty is shown in Figure 8 for the optical system with 50km long optical fiber. The shape of the photodiode bandwidth penalty is typical in Figure 8. If the photodiode bandwidth is high enough, the photodiode would be able to produce the stationery values of the output signal before the end of the pulsewidth, and the photodiode bandwidth penalty would be 0 (for $d < 3.5\,\mu$m). For $d > 3.5\,\mu$m the bandwidth is low enough to "cut" and disable the stationery values in the photodiode output signal. Hence, the photodiode bandwidth penalty is greater than zero.

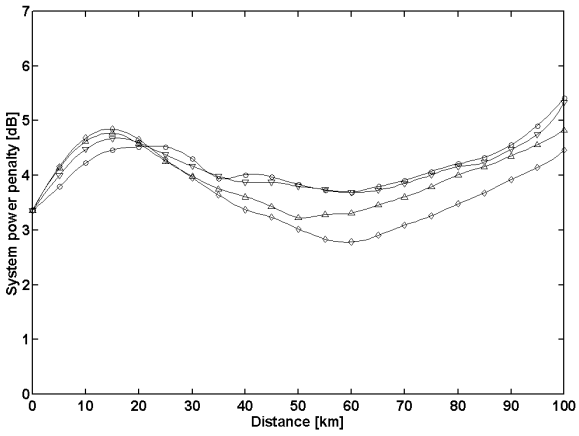

Fig. 7. System power penalty for different P-i-N photodiode parameters: ideal-square law detector (○), P-i-N photodiode with $d = 2.5\mu$m (▽), $d = 4\mu$m (△), $d = 5.5\mu$m (◇). Extinction ratio $r_{ext} = 2.75 : 1$ is equivalent to the extinction ratio penalty $P_E = 3.31$ dB.

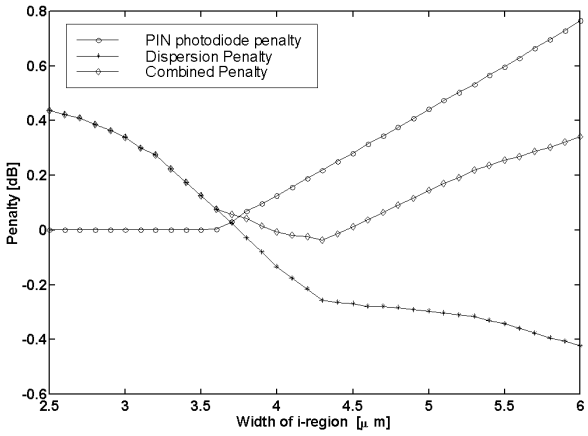

Fig. 8. Combined dispersion and P-i-N photodiode bandwidth penalty. Extinction ratio is $r_{ext} = 2.75 : 1$, while the length of the optical fiber is 50km.

Dispersion penalty decreases as i-region width increases. Combined dispersion and photodiode bandwidth penalty represents the sum of these two components and has the minimum for $d = 4.3\,\mu$m. This value of i-region width appears to be optimal concerning the given constraints. Similar results can be obtained for various sets of parameters. It should be noted that the dispersion and photodiode bandwidth penalties can be also combined with the extinction ratio penalty and speed penalty, which have been not considered due to simplicity.

IV. Conclusion

Our analysis gives us possibilities to derive the following conclusions:

- We have described developed model of the InGaAs P-i-N photodiode which can be used for the determination of the pulse response of P-i-N photodiode in various operating regimes, especially for small incident energies of radiation. The most important aspects of carrier dynamics are included in this model.
- This model has been successfully implemented, as the part of the more complex mathematical model, in the computer simulator of 10 Gb/s 1.55 μm IM/DD digital optical system with InGaAs P-i-N photodiode as an optical receiver. Our simulations give more accurate results then those from the literature, because the stronger filtering of the propagating signal and finite bandwidth of the P-i-N photodiode are accounted in the analysis.

• Since the limited photodiode bandwidth may cause negative dispersion penalty, we introduced the photodiode bandwidth penalty in order to model more precisely the influence of the P-i-N photodiode on system power penalty. The analysis has shown that the combined dispersion and photodiode bandwidth penalty has the local minimum which appears suitable for the system operation.

Presented computer simulator emerges as an excellent optimization tool for 1.55μm lightwave system.

References

[1] P. J. Corvini and T. L. Coch, "Computer Simulation of High-Bit-Rate Optical Fiber Transmission Using Single-Frequency Laser", *Journal of Lightwave Technology*, Vol. 5, No. 11, 1987, pp. 1591-1595

[2] J. Cartledge and G. Burley, "The effect of Laser Chirping on Lightwave System Performance", *Journal of Lightwave Technology*, Vol. 7, No. 3, 1989, pp. 568-573

[3] P. Lau and T. Makino, "Effects of Laser Diode Parameters on Power Penalty in 10 Gb/s Optical Fiber Transmission Systems", *Journal of Lightwave Technolgy*, Vol. 15, No. 9, 1997, pp. 1663-1668

[4] R. D. Esman and K. J. Williams, "Measurement of Harmonic Distortion in Microwave photodiodes", IEEE Photonic Technology Letters, Vol. 2, No. 7, 1990, pp. 502-504

[5] M. Dentan and B. de Cremouxs, "Numerical simulation of the nonlinear respons of the P-i-N photodiode under high illumination", *IEEE Journal of Lightwave Technology*, Vol. 8, No. 8, 1990, pp. 1137-1144

[6] K. J. Williams and R. D. Esman, "Observation of photodiode Nonlinearities", Electronics Letters, Vol. 28, No. 8, 1992, pp. 731-732

[7] R. Sabella and S. Merli, "Analysis of InGaAs P-i-N photodiode frequency response", IEEE Journal of Quantum Electronics, Vol. 29, No. 3, 1993, pp. 906-916

[8] R. R. Hayes and D. L. Persechini, "Nonlinearity of pin Photodtectors", IEEE Photonics Technology Letters, Vol. 5, No. 1, 1993, pp. 70-72

[9] J. Radunović and D. Gvozdić, "Nonstationary and Nonlinear Response of a P-i-N photodiode Made of a Two-Valley Semiconductor", *IEEE Transaction of Electron Devices*, Vol. 40, No. 7, 1993, pp.1238-1244

[10] K. J. Williams, R. D. Esman, M. Dagenais, "Nonlinearities in P-i-N Microwave photodiodes", *IEEE Journal of Lightwave Technology*, Vol. 14, No. 1, 1996, pp. 84-96

[11] P. Matavulj, D. Gvozdić, J. Radunović, J. Elazar, "Nonlinear Pulse Response of P-i-N photodiode Caused by the Change of the Bias Voltage", Int. J. Infrared & Millimeter Waves, Vol. 17, No. 9, 1996, pp. 1519-1528

[12] P. Matavulj, D. Gvozdić, J. Radunović "Influence of Nonstationary Carrier Transportion on the Bandwidth of P-i-N photodiode", *Journal of Lightwave Technology*, Vol. 15 No. 12, 1997, pp. 2270-2277

[13] S. Mohrdiek, H. Burkhard, F. Steinhagen, H. Hillmer, R. Lösch, W. Schlapp and R. Göbel, "10-Gb/s Standard Fiber Transmission Using Directly Modulated 1.55-μm Quantum-Well DFB Lasers", *IEEE Photonic Technology Letters*, Vol. 7, No. 11, 1995, pp. 1357-1359

[14] G. P. Agrawal, *Nonlinear fiber optics*, Academic Press, New York, 1989

[15] B. E. A. Saleh and M. I. Irshid, "Coherence and Intersymbol Interference in Digital Fiber Optic Communication Systems", *IEEE Journal of Quantum Electronics*, Vol. 18, No. 6, 1982, pp. 944-951

[16] K. Vuorinen, F. Gaffiot and G. Jacquemod, "Modeling Single-Mode Lasers and Standard Single-Mode Fibers Using a Hardware Description Language", *IEEE Photonic Technology Letters*, Vol. 9, No. 6, 1997, pp. 824-826

[17] M. Jackson and G. Burley, "Modeling dispersive fibers with a circuit simulator", *Electronics Letters*, Vol. 30, No. 15, 1994, pp. 1245-1246

[18] A. F. Elrefarie, R. E. Wagner, D. A. Atlas and D. G. Daut, "Chromatic Dispersion Limitations in Coherent Lightwave Transmission Systems", *Journal of Lightwave Technology*, Vol. 6, No. 5, 1988, pp. 704-709

[19] J. Binder and U. Kohn, "10 Gbit/s-Dispersion Optimized Transmission at 1.55 μm Wavelength on Standard Single Mode Fiber", *IEEE Photonic Technology Letters*, Vol. 6, No. 4, 1994, pp. 558-560

[20] M. Cvetković, P. Matavulj, J. Radunović and A. Marinčić, "Analysis of the Finite-Impulse-Response (FIR) Filters Implementation in the Modeling of the Single-mode Optical Fiber", in Proc. IEEE TELSIKS'99, Niš, Yugoslavia, Oct,13-15.1999, Vol.1, pp. 325-328

[21] M. Cvetković, P. Matavulj, J. Radunović and A. Marinčić, "Analysis of the High Bit-rate 1.55 μm Lightwave System with the Limited P-i-N Photodiode Bandwidth", in Proc. IEEE MIEL'99, Niš, Yugoslavia, 2000, in press.

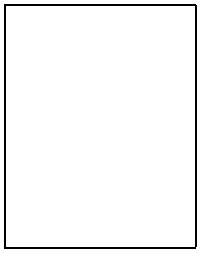

Mladen Cvetković was born in Belgrade, Yugoslavia in 1968. He received B.S. and M.S. Degree in 1992. and 1996, respectively, from the Faculty of Electrical Engineering, University of Belgrade, Yugoslavia. His research interests are the modeling and characterization of the optoelectronic devices and optical communication systems.

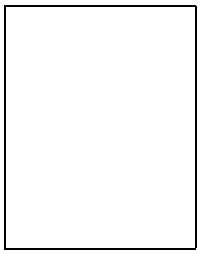

Petar Matavulj was born in Gradiška, Srpska Republic, in 1971. He received the B.S. degree in 1994 and the M.S. degree in 1997, both in electrical engineering from the Belgrade University, Belgrade, Yugoslavia. In 1994. he joined the Faculty of Electrical Engineering, University of Belgrade, where he is now an Assistant of Physical Electronics. He is currently working towards the Ph.D. degree in electrical engineering at the Belgrade University. His research interests are modeling, simulation and characterization of high-speed optoelectronic devices, lightwave system modeling and fiber optics sensors.

He is a student member of the IEEE Laser and Electro-Optics Society and IEEE Electron Devices Society.
E-mail: matavulj@kiklop.etf.bg.ac.yu

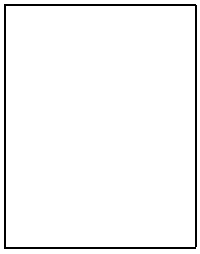

Jovan Radunović was born in Priština, Serbia, Yugoslavia in 1949. He received the M.S. degree in 1977 and the Ph.D. degree in 1984, both in electrical engineering from the Belgrade University, Belgrade, Yugoslavia. In 1974. he joined the Faculty of Electrical Engineering, University of Belgrade, where he is now a Professor of Physical Electronics. His research areas include fundamental studies of kinetic fluctuations in semiconductors, electron transport in semiconductors, and modeling and simulation of high-speed semiconductor devices.
E-mail: radunovic@buef31.etf.bg.ac.yu

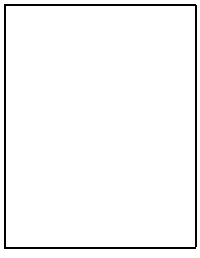

Aleksandar Marinčić received B.Sc. and P.G.D. degree from Faculty of Electrical Engineering, Belgrade, Yugoslavia and Ph.D. degree from Sheffield University, Great Britain in 1956, 1957 and 1961, respectively. He joined Faculty of Electrical Engineering in Belgrade in 1958 until 1967, when he joined M.E.Technical University in Ankara, Turkey as a visiting professor and UNESCO expert. From 1971 to 1974 he was with Electronic Faculty of Niš, Yugoslavia, and in 1974 he returned to Faculty of Electrical Engineering in Belgrade, where he is now emeritus professor in telecommunications. His main research areas are microwaves and optical communications, the fields in which he published several books and numerous papers. He also participated and led several national and international research projects. He is corr.member of the Serbian Academy of Sciences and Arts, full member of Engineers Academy of Yugoslavia and IEEE member. He was for 14 years director of Nikola Tesla Museum in Belgrade.